



## **Altering Plasmonic Nanoparticle Size Through Thermal Annealing for Improved Photovoltaic Devices**

**by Rukshan Fernando, Fred Semendy, and Priyalal Wijewarnasuriya**

---

**ARL-TR-5895**

**January 2012**

## **NOTICES**

### **Disclaimers**

The findings in this report are not to be construed as an official Department of the Army position unless so designated by other authorized documents.

Citation of manufacturer's or trade names does not constitute an official endorsement or approval of the use thereof.

Destroy this report when it is no longer needed. Do not return it to the originator.

# **Army Research Laboratory**

Adelphi, MD 20783-1197

---

---

**ARL-TR-5895**

**January 2012**

---

---

## **Altering Plasmonic Nanoparticle Size Through Thermal Annealing for Improved Photovoltaic Devices**

**Rukshan Fernando**  
University of California Irvine, CA 92697

**Fred Semendy and Priyalal Wijewarnasuriya**  
Sensors and Electron Devices Directorate, ARL

# REPORT DOCUMENTATION PAGE

*Form Approved*  
OMB No. 0704-0188

Public reporting burden for this collection of information is estimated to average 1 hour per response, including the time for reviewing instructions, searching existing data sources, gathering and maintaining the data needed, and completing and reviewing the collection information. Send comments regarding this burden estimate or any other aspect of this collection of information, including suggestions for reducing the burden, to Department of Defense, Washington Headquarters Services, Directorate for Information Operations and Reports (0704-0188), 1215 Jefferson Davis Highway, Suite 1204, Arlington, VA 22202-4302. Respondents should be aware that notwithstanding any other provision of law, no person shall be subject to any penalty for failing to comply with a collection of information if it does not display a currently valid OMB control number.

**PLEASE DO NOT RETURN YOUR FORM TO THE ABOVE ADDRESS.**

<b>1. REPORT DATE (DD-MM-YYYY)</b> January 2012		<b>2. REPORT TYPE</b> Final		<b>3. DATES COVERED (From - To)</b>	
<b>4. TITLE AND SUBTITLE</b> Altering Plasmonic Nanoparticle Size Through Thermal Annealing for Improved Photovoltaic Devices				<b>5a. CONTRACT NUMBER</b>	
				<b>5b. GRANT NUMBER</b>	
				<b>5c. PROGRAM ELEMENT NUMBER</b>	
<b>6. AUTHOR(S)</b> Rukshan Fernando, Fred Semendy, and Priyalal Wijewarnasuriya				<b>5d. PROJECT NUMBER</b>	
				<b>5e. TASK NUMBER</b>	
				<b>5f. WORK UNIT NUMBER</b>	
<b>7. PERFORMING ORGANIZATION NAME(S) AND ADDRESS(ES)</b> U.S. Army Research Laboratory ATTN: RDRL-SEE-I 2800 Powder Mill Road Adelphi, MD 20783-1197				<b>8. PERFORMING ORGANIZATION REPORT NUMBER</b>  ARL-TR-5895	
<b>9. SPONSORING/MONITORING AGENCY NAME(S) AND ADDRESS(ES)</b>				<b>10. SPONSOR/MONITOR'S ACRONYM(S)</b>	
				<b>11. SPONSOR/MONITOR'S REPORT NUMBER(S)</b>	
<b>12. DISTRIBUTION/AVAILABILITY STATEMENT</b> Approved for public release; distribution unlimited.					
<b>13. SUPPLEMENTARY NOTES</b>					
<b>14. ABSTRACT</b> We created gold (Au) and silver (Ag) nanoparticles by e-beam deposition on an n-type silicon substrate followed by rapid thermal annealing (RTA) under nitrogen gas. Thermal annealing was performed in two ways: first by varying temperature for a constant time and second by varying time at a constant temperature. RTA under the right eutectic temperature, which varies metal to metal, should create nano-metal particles on the substrate. These nanoparticles were characterized by optical spectroscopy and atomic force microscopy (AFM). Results from the optical measurements provide information on the reflective and absorptive characteristics of Au and Ag nanoparticles. AFM provided additional information about the surface properties including size, density distribution, and other relevant values. Results are reported here and they indicate the nature of the Au and Ag nanoparticles by their optical and surface characterization. We propose that the absorption properties can be obtained in solar cells by exploiting the plasmonic behavior of these nanoparticles.					
<b>15. SUBJECT TERMS</b> Plasmonic nanoparticles, thermal annealing, photovoltaic devices					
<b>16. SECURITY CLASSIFICATION OF:</b>			<b>17. LIMITATION OF ABSTRACT</b>  UU	<b>18. NUMBER OF PAGES</b>  22	<b>19a. NAME OF RESPONSIBLE PERSON</b> Fred Semendy
<b>a. REPORT</b> Unclassified	<b>b. ABSTRACT</b> Unclassified	<b>c. THIS PAGE</b> Unclassified			<b>19b. TELEPHONE NUMBER (Include area code)</b> (301) 394-4627

---

## Contents

---

<b>List of Figures</b>	<b>iv</b>
<b>List of Tables</b>	<b>iv</b>
<b>Acknowledgments</b>	<b>v</b>
<b>1. Introduction</b>	<b>1</b>
<b>2. Experimental Procedures</b>	<b>3</b>
<b>3. Results and Discussion</b>	<b>7</b>
<b>4. Conclusion</b>	<b>10</b>
<b>5. References</b>	<b>11</b>
<b>List of Symbols, Abbreviations, and Acronyms</b>	<b>12</b>
<b>Distribution List</b>	<b>13</b>

---

## List of Figures

---

Figure 1. Plasmonic solar cell using metal nanoparticles on Si substrate. ....	1
Figure 2. (a) CHA E-beam evaporation machine procedure and (b) deposition process for 20-Å Au/Ag particle formation on Si surface, deposited at $1.7 \times 10^{-6}$ Torr at $0.3 \text{ \AA/s}$ . ....	4
Figure 3. RTA process used for experiment. ....	5
Figure 4. Picture of Perkin Elmer Lambda 950 UV-Vis spectrometer used for optical measurements. ....	7
Figure 5. (a) Reflection of Ag with time variable samples and (b) absorption of Ag with temperature variable samples. ....	8
Figure 6. AFM pictures of step height analysis of Au and Ag samples. ....	9
Figure 7. AFM surface plots of samples with corresponding rms values. ....	9

---

## List of Tables

---

Table 1. With the eutectic temperature for Au being $389 \text{ }^\circ\text{C}$ and $205 \text{ }^\circ\text{C}$ for Ag the following samples were annealed accordingly. ....	6
Table 2. Other nanoparticle size measurements acquired from AFM analysis. ....	10

---

## **Acknowledgments**

---

Rukshan Fernando wishes to acknowledge the assistance of Dr. Fred Semendy, Dr. Priyalal Wijewarnasuriya, and Gregory Meissner of the U.S. Army Research Laboratory.

INTENTIONALLY LEFT BLANK.

---

## 1. Introduction

---

Photovoltaics is a method of generating electrical power by converting solar radiation into direct current electricity using semiconductors that use the photovoltaic effect (1). Thin-film solar cells are a new design approach for photovoltaic devices. Photovoltaic cells are made of special materials called semiconductors, such as silicon (Si), which is currently the most commonly used material. Basically, when light strikes a cell, a certain portion of it is absorbed within the semiconductor material, which means that the energy of the absorbed light is transferred to the semiconductor itself. This process is shown in figure 1. The transferred energy knocks the electrons loose, allowing them to flow freely. Photovoltaic cells have one or more electric fields that act to force electrons freed by light absorption to flow in a certain direction (2). This flow of electrons is called a current, and by placing metal contacts on the top and bottom of the photovoltaic cell, we can draw that current off for external use in which there are thousands of applications in the U.S. Army.

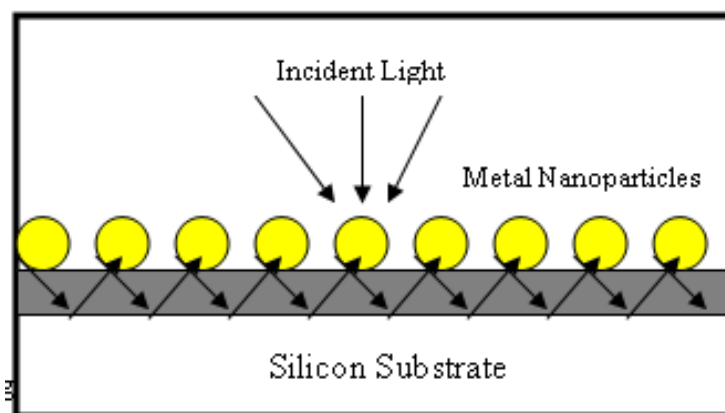


Figure 1. Plasmonic solar cell using metal nanoparticles on Si substrate.

One problem is that pure crystalline Si is a poor conductor of electricity because none of the electrons are free to move around (3). To help with this issue, the Si in a solar cell has impurities. The process of purposely adding impurities is called doping, in which the resulting Si is called n-type because of the prevalence of free electrons. N-type doped Si, which is used for this experiment, is a much better conductor than pure Si (4). However, in this experiment, we are dealing with thin-film solar cells and the biggest problem for thin-film solar cells is that they don't absorb as much light as the current solar cells do.

Methods for trapping light on the surface or in the solar cell are crucial in order to make thin-film solar cells. One method that has been explored over the past few years is to scatter light using metal nanoparticles excited at their surface plasmon resonance (5). This allows light to be absorbed more directly without the relatively thick additional layer required in other types of

thin-film solar cells. In recent years, plasmonic nanoparticles closely adhered to absorbing semiconductors have been used to enhance absorption in ultrathin-film solar cells (6). When light hits these metal nanoparticles at their surface plasmon resonance, the light is scattered in many different directions. This allows light to travel along the solar cell and bounce between the substrate and the metal nanoparticles, enabling the solar cells to absorb more light (7).

Observing the relationship between the size of the nanoparticles and the detection or absorption of the particles is an important concept in plasmonic research. In this experiment we deposited metal nanoparticles of gold (Au) and silver (Ag) on the top surface of a thin-film solar cell, and focused on characterizing the optical properties of the plasmonic nanoparticles and determining how much the absorption sensitively depends on the nanoparticles size and shape and whether this can be altered by thermal annealing.

In this experiment, metal particles were deposited from CHA E-beam evaporation. The samples were then thermally annealed using rapid thermal annealing (RTA) to create nanoparticles. We chose RTA over other methods for creating nanoparticles, such as inert-gas condensation and chemical synthesis. Inert-gas condensation is frequently used to make nanoparticles from metals with low melting points. The metal is vaporized in a vacuum chamber and then super-cooled with an inert gas stream. The super-cooled metal vapor then condenses into nanometer-sized particles, which can be entrained in the inert gas stream and deposited onto a substrate. Chemical synthesis, specifically, sol-gel processing, is a wet chemical synthesis process used to generate nanoparticles by gelation, precipitation, and hydrothermal treatment. The advantage to creating nanoparticles using RTS is that it is much faster than any other method, including inert-gas condensation, and thus, due to time constraints within the research effort, we deemed it the best choice.

We created these nanoparticles, grown on Si substrates, for testing and examination. Si is the chosen best material for the photovoltaic application substrates because of its low cost, abundance in nature, long-term stability, nontoxicity, and well-established technology.

The absorption of the applied light onto the nanoparticles grown on the substrate depends on each particle's size. Metallic particles that are much smaller than that of the wavelength of light usually absorb more. Many researchers have looked into this new development, one of whom being S. Pillai (8). Pillai has done research in which Ag nanoparticles were deposited onto a Si wafer on an insulator. He has demonstrated absorption and emission enhancement from Si solar cells by using the nanoscale properties of metals. He targeted enhancement close to the bandgap of Si, where absorption is weak. For his experiment, metal nanoparticles were deposited by thermal evaporation of thin layers, which was then followed by thermal annealing. The Ag nanoparticles shape was tuned by a thermal annealing at temperatures well below the melting point of Ag. Then due to surface tension, the particles merge together to form islands. This process is one of the simplest ways to deposit metal nanoparticles onto a substrate. After running the experiment it was concluded that for front surface application, smaller metal particles provide

maximum enhancement in the visible (Vis) as well as the near-infrared (NIR), but larger particles would be more beneficial from both thin and thick light-emitting diodes (LEDs) (9). Thin-film solar cells have the potential to significantly decrease the cost of photovoltaic devices. Light trapping is very critical in thin-film crystalline Si solar cells in order to increase light absorption and cell efficiency (10). High efficiency solar cell design needs optically thick photovoltaic layers to give nearly complete light absorption, as well as minority carrier diffusion lengths many times the material thickness to allow efficient carrier collection (11).

---

## 2. Experimental Procedures

---

The Au and Ag layers were deposited onto double side polished (DSP) <100> Si substrates using a CHA E-beam evaporator. The two separate Si wafer substrates used for each metal deposition were also n-type, meaning they had negative-type doping. Electron beam evaporation is a form of physical vapor deposition in which a target anode is bombarded with an electron beam given off by a charged tungsten filament under high vacuum. The electron beam causes atoms from the target to transform into the gaseous phase. These atoms then precipitate into solid form, coating everything that is in the vacuum chamber with a thin layer of the anode material. The E-beam evaporation process is shown in figure 2a. The goal was to deposit only 20 Å of Au and 20 Å of Ag onto the other, because this would ensure a more uniform layer of particles. The process of depositing metal nanoparticles onto the Si substrate is shown in figure 2b. In order to work properly with best results, the pressure in the CHA evaporator was maintained below  $1.7 \times 10^{-6}$  Torr. The Au and Ag metal particles were deposited separately and evaporated onto the substrate at a rate of 0.3 Å/s to ensure an even layer of particles on the surface. All of the deposition procedures were done in the U.S. Army Research Laboratory (ARL) cleanroom.

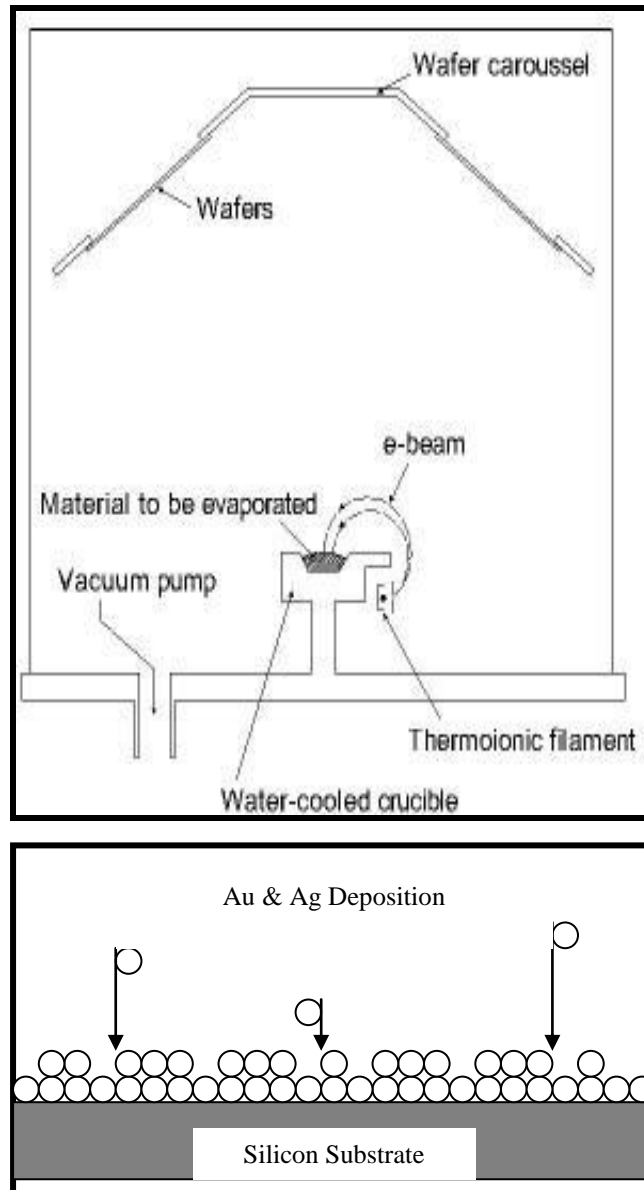


Figure 2. (a) CHA E-beam evaporation machine procedure and (b) deposition process for 20-Å Au/Ag particle formation on Si surface, deposited at  $1.7 \times 10^{-6}$  Torr at  $0.3 \text{ \AA/s}$ .

The Au and Ag deposited wafers were then cleaved in which the goal was to have 12 identical-sized samples of Si-Au and 12 identical-sized samples of Si-Ag. First the Si substrate was measured and lined up to be cut into identical 2x2 cm pieces with a diamond tip pen. Then the Si wafer was simply cleaved by snapping and breaking the pieces along the inscribed lines. The samples were then cleaned using basic lab cleaning procedures. First, each sample was washed with acetone and then with isopropyl alcohol (IPA). Then, the samples were rinsed off with de-ionized water and finally blow dried with a nitrogen gun. Both the Si-Au and Si-Ag were cleaved and cleaned in the same manner.

Samples were then annealed in the rapid thermal annealer. RTA is a process used in semiconductor device fabrication, which consists of heating a single wafer at a time in order to affect its electrical properties. Unique heat treatments are designed for different effects. The RTA process is performed by equipment that heats a single wafer at a time using lamp-based heating and a hot plate that a wafer is brought near. The wafer is heated by lamps located on top and below the sample holder and the pyrometer is used to determine the temperature of the sample's surface, which is shown in figure 3. Unlike furnace anneals, they are short in duration, processing each wafer in several minutes. For this experiment, RTA was used to create the nanoparticles only, but wafers can also be heated to activate dopants, change film-to-film or film-to-wafer substrate interfaces, densify deposited films, change states of grown films, and even repair damage from ion implantation. During cooling, however, wafer temperatures must be brought down slowly so they do not break due to thermal shock. To achieve short-time annealing, the trade off is made in temperature and process uniformity, temperature measurement and control, and wafer stress as well as throughput. One main problem with the RTA process is keeping the wafer at a constant temperature. The annealing temperature usually shoots up 10–20 °C above the needed temperature during the process, which affects the consistency of the resulted samples. To avoid this problem, a trial run was conducted with a blank sample in between each process and the power of the machine was adjusted according to the needed temperature.

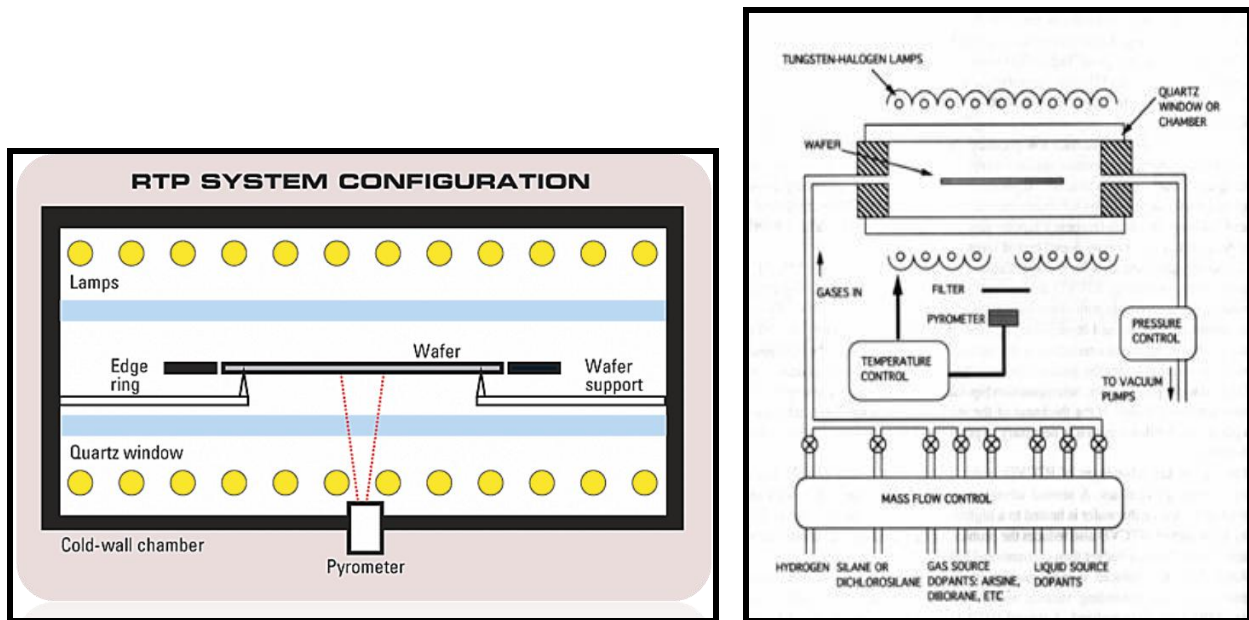


Figure 3. RTA process used for experiment.

Each 2x2 cm sample was annealed at a different temperature and for a different amount of time for each sample. Annealing under the right eutectic temperature for Au, which is 389 °C, and Ag, which is 210 °C, should create nano-metal particles on the substrate. Six samples of Au were annealed from 250 to 500 °C with a temperature difference of 50 °C in between each sample at a

constant time of 30 min. Then a separate six samples of Au were annealed from 10 to 110 min with a time difference of 20 min in between each annealing process at a constant temperature of 450 °C. Five samples of Ag were annealed from 200 to 400 °C with a difference of 50 °C in between each annealing at a constant time of 50 min. Finally, a separate five samples of Ag were annealed from 30 to 70 min with a time difference of 10 min in between each annealing process at constant temperature of 250 °C. The process for each individual sample is shown in table 1. To start the RTA process, nitrogen gas is turned on to 4 psi for lamp cooling and RTA is switched on. The Set II temperature, which is the temperature at which the process begins, is always set to 150 °C and the Set I temperature is set to the maximum temperature that is needed for the specific sample. By placing each sample metal side up onto the annealing wafer and setting the timer to the needed time, the samples were annealed.

Table 1. With the eutectic temperature for Au being 389 °C and 205 °C for Ag the following samples were annealed accordingly.

Au (20Å) [Time Constant]			Ag (20Å) [Temp Constant]			Ag (20Å) [TimeConstant]			Au (20Å) [Temp Constant]		
Sample	Temp (°C)	Time (min)	Sample	Temp (°C)	Time (min)	Sample	Temp (°C)	Time (min)	Sample	Temp (°C)	Time (min)
A1	250	30	B1	250	30	A1	200	50	B1	450	10
A2	300	30	B2	250	40	A2	250	50	B2	450	30
A3	350	30	B3	250	50	A3	300	50	B3	450	50
A4	400	30	B4	250	60	A4	350	50	B4	450	70
A5	450	30	B5	250	70	A5	400	50	B5	450	90
A6	500	30							B6	450	110

The annealed samples were used for optical measurements, which include the reflection, transmission, and absorption of the samples. To test the performance of the nanoparticles on the substrate, the optical measurements were obtained by using the Perkin Elmer 950 ultraviolet (UV)-Vis-NIR spectrometer. For testing the transmission of each sample, the auto-zero, or a blank, was done for reference and to calibrate the spectrometer to ensure maximum accuracy before testing each sample. After performing the auto-zero, the samples were tested. When making transmission measurements, the spectrometer quantitatively compares the fraction of light that passed through the reference, or blank test, and the test sample. For reflectance measurements, the auto-zero or reference is calculated by a 100% reflective mirror. Then, the spectrometer quantitatively compares the fraction of light that reflects from the reference mirror and the test samples. Figure 4 shows the process of how the spectrometer collects data for transmission and reflection. The transmission and reflection data were measured between wavelengths of 400–1200 nm, using the spectrometer by positioning each sample to the holder.

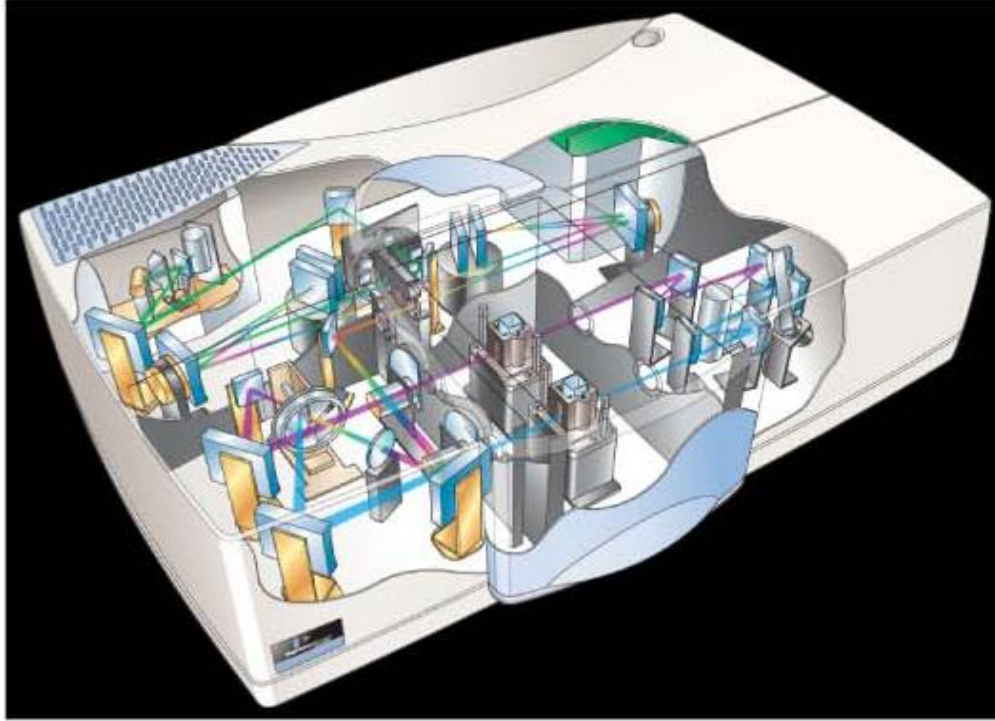


Figure 4. Picture of Perkin Elmer Lambda 950 UV-Vis spectrometer used for optical measurements.

The samples were then examined using atomic force microscopy (AFM), which was used to examine the physical properties of the nanoparticles. AFM consists of a cantilever with a sharp tip at its end that is used to scan the surface of the substrate. The cantilever is typically Si or silicon nitride with a tip radius of curvature in order of nanometers. When the tip is brought onto a sample surface, forces between the tip and the sample lead to a deflection of the cantilever according to Hooke's law. AFM has many advantages over the scanning electron microscope (SEM). Unlike the SEM, which provides a two-dimensional projection of a sample, AFM can provide a three-dimensional surface profile.

---

### 3. Results and Discussion

---

The data collected from the annealed samples were examined with the spectrometer and were measured by shooting light at each sample between wavelengths of 400–1200 nm. The spectrometer gives data between the wavelength of the light that is applied to the surface and the effect it has with the surface of each sample. Graphs for each time-dependent and temperature-dependent sample were plotted using Microsoft Excel. After calculating the reflection and transmission of each sample and graphing the data with respect to the wavelength, the absorption was calculated by using the following formula and were graphed:

$$\%A = 1 - (\%T + \%R) \quad (1)$$

The reflection and absorption data are plotted in figure 5a and b. According to the graph data, as the size of the Ag nanoparticles increased, the reflection of each sample also increased but for also with large particle size there tends to be a reduction in absorption at shorter wavelengths. Also, there is an increase in absorption with large particles at longer wavelengths. From the graphs, smaller particles also show to be less reflective than the larger particles.

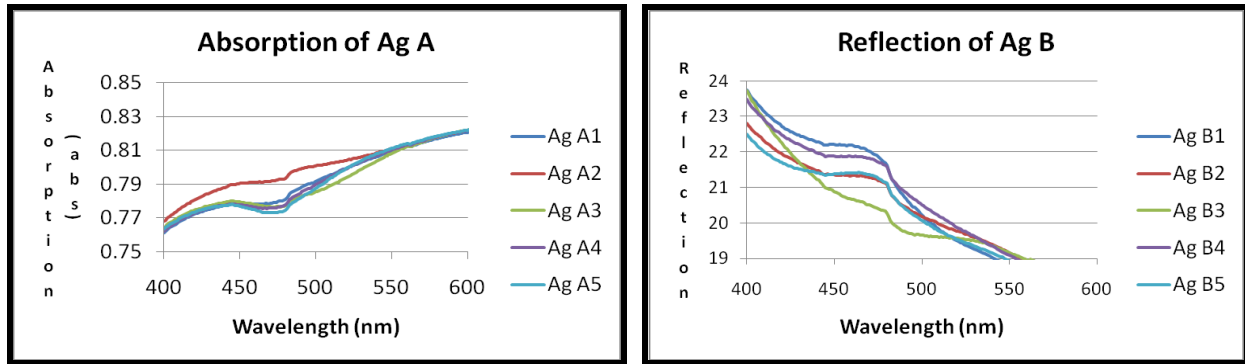


Figure 5. (a) Reflection of Ag with time variable samples and (b) absorption of Ag with temperature variable samples.

The samples were then examined using AFM, which was used to examine the physical properties of the nanoparticles. Samples A1, A3, A5, B1, and B5 from the Ag samples and samples A1 and A3 from Au were chosen to be used for AFM. However, first, each sample had to be fit into AFM device and thus were measured, lined up, and cut into identical 1x1 cm pieces with a diamond tip pen. Then, the samples were simply cleaved by snapping and breaking the pieces along the inscribed lines. After that, they were cleaned using basic lab cleaning procedures.

The AFM procedure helps to see the actual size of each nanoparticle and make a relationship between the nanoparticles size and the data from the spectrometer. AFM can analyze many types of data such as the step height, bearing depth, depth, grain size, particle analysis, roughness, and section analysis of each sample. Of the measurements that AFM can provide, step height analysis is very important, because it provides information about the height of sample. The step height measurements of each sample are shown in figure 6. This is necessary because the curvature of the substrate might well be sufficient to prevent the use of the simple least-squares line fit. When measured, the step and substrate areas are treated as line segments, allowing the curvature of the substrate to be removed, resulting in a straight-line representation of the substrate. The step heights are calculated from this line in the areas adjacent to each step.

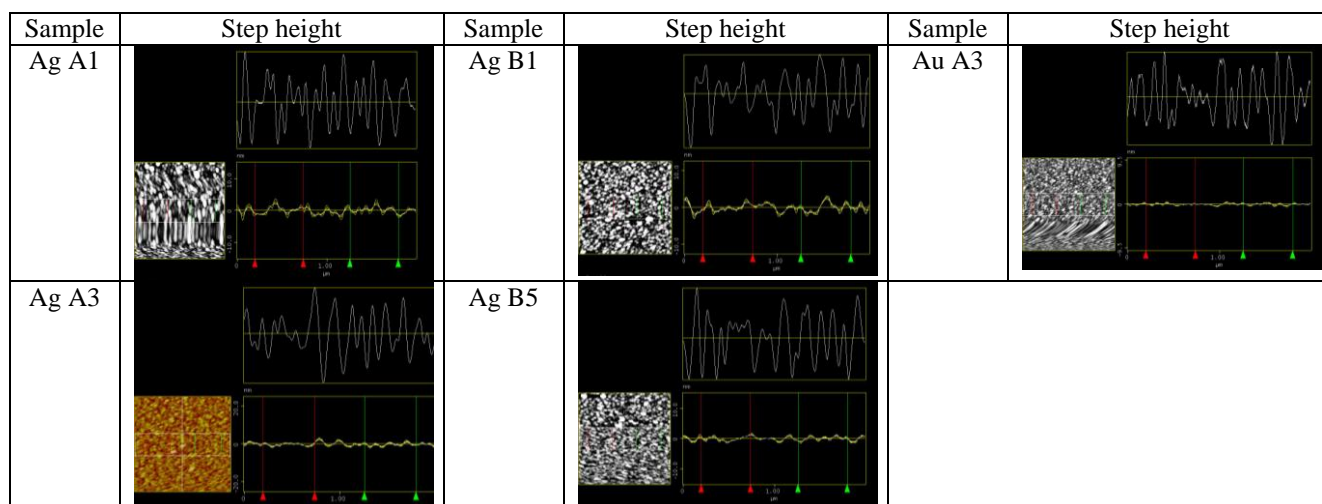


Figure 6. AFM pictures of step height analysis of Au and Ag samples.

The scanned area was  $2 \mu\text{m} \times 2 \mu\text{m}$  and the root mean squared (rms) values were obtained. Figure 7 shows the AFM surface plots of the samples that were analyzed. The first one are Ag nanoparticles on Si annealed at  $200 \text{ }^\circ\text{C}$  with a density of  $3.7 \times 10^{10}$  per  $\text{cm}^2$ . Sample Ag A3 has been annealed at  $300 \text{ }^\circ\text{C}$ , which is higher than the  $200 \text{ }^\circ\text{C}$  at which sample Ag A1 was annealed. Sample Ag A1 exhibits smaller-sized nanoparticles of Ag than sample Ag A3. The rms values of each sample also noticeably increases as the temperature and time at which they are annealed increases.

Sample	AFM Roughness	rms Value	Sample	AFM Roughness	rms Value	Sample	AFM Roughness	rms Value
Ag A1		2.75 nm	Ag B1		3.64 nm	Au A3		1.075 nm
Ag A3		3.067 nm	Ag B5		3.687 nm			

Figure 7. AFM surface plots of samples with corresponding rms values.

Table 2 lists the bearing depth, grain height, and particle height of the scanned samples. The bearing depth, which is presented by average height in bearing area, is seen here as increasing for the annealed samples. The grain height, which measures the height of each individual grain, is also shown as growing for the annealed samples. The particle height, which is a measurement of

the height of each, also increases. A trend in increasing value is seen in the results as the annealing process changes for each sample. The more a sample is annealed, whether it is increase of the temperature or the annealed time, the physical property values also increase.

Table 2. Other nanoparticle size measurements acquired from AFM analysis.

<b>Sample</b>	<b>Bearing Depth (nm)</b>	<b>Grain Height (nm)</b>	<b>Particle Height (nm)</b>
Ag A1	9.261	2.378	13.824
Ag A3	16.197	12.293	15.916
Ag B1	18.309	11.339	13.69
Ag B5	22.845	15.019	25.294
Au A3	4.095	2.712	5.235

---

## 4. Conclusion

---

We investigated the optical and physical properties of Au and Ag nanoparticles grown on a Si substrate. The reflection, transmission, and absorption of Au and Ag nanoparticles were deposited onto Si wafers that were altered by different processes of thermal annealing. The size of the nanoparticles on each sample changed in each different case. It is evident that as the temperature and time, at which the thermal annealing occurred, the Au and Ag nanoparticle grew larger in size and the reflection, transmission and absorption also changed as the particles grew. The obtained results show that for front surface application, smaller metal particles provide maximum enhancement for visible detection. With large particle size, there tends to be a reduction in absorption at shorter wavelengths; however, there is an increase in absorption with large particles at longer wavelengths. From the graphs, the larger particles were also shown to be more reflective than the smaller particles.

Through this work, we have shown that metal nanoparticles created by thermal annealing can change the physical and optical properties of the nanoparticles. Enhancing these nanoparticles can help to improve the conversion efficiency of solar cells if metal nanoparticles are included in the photovoltaic devices.

---

## 5. References

---

1. Nakayama, K.; Tanabe K.; Atwater, H. Plasmonic Nanoparticle Enhanced Light Absorption in GaAs Solar Cells. *Journal of Appl. Physics* **2008**, *93*, 121904-1.
2. Atwater, H.; Polman, A. Plasmonics for Improved Photovoltaic Devices. *Nature Material: Review Article* **2010**, 205–208.
3. Pillai, S.; Catchpole, K. R.; Trupke, T.; Green, M. A. Surface Plasmon Enhanced Silicon Solar Cells. *Applied Physics* **2007**, *101*, 1–6.
4. Popok, V. N.; Gromov, A. V.; Nuzhdin, V. I.; Stepanov, A. L. Optical and AFM Study of Ion-synthesized Silver Nanoparticles in Thin Surface Layers of SiO<sub>2</sub> Glass. *Journal of Non-Crystalline Solids* **2010**, *35*, 1259.
5. Chen, F.; Johnston, R. L. Plasmonic Properties of Silver Nanoparticles on Two Substrates. *Springer Science: Plasmonics* **2009**, 147–148.
6. Okumu, J.; Dahmen, C.; Luysberg, M.; Wuttig, M. Photochromic Silver Nanoparticles Fabricated by Sputter Deposition. *Journal of Appl. Physics* **2005**, *97*, 1–2.
7. Ferry, V.; Verschuuren, M.; Li, H.; Verhagen, E.; Atwater, H.; Polman, A.; Walters, R. Light Trapping in Ultrathin Plasmonic Solar Cells. *Optics Express* **2010**, *18* (7), 5–7.
8. Lojek. B. Early History of Rapid Thermal Processing. *ATMEL Corporation* **2005**, 3–10.
9. Beck, F. J.; Mokkalapati, S.; Catchpole, K. R. Plasmonic Light-trapping for Si Solar Cells using Self-assembled, Ag Nanoparticles. *Progress in Photovoltaics*. **2010**, *18* (7), 501–502.

---

## List of Symbols, Abbreviations, and Acronyms

---

%R	percent reflection
%T	percent transmission
AFM	atomic force microscopy
Ag	silver
Au	gold
DSP	double sided polish
IPA	isopropyl alcohol
NIR	near infrared
Vis	visible
UV	ultraviolet
nm	nanometers
n-type	negative type
rms	root mean squared
RTA	rapid thermal annealing
SEM	scanning electron microscope
Si	silicon

NO. OF COPIES	ORGANIZATION	NO. OF COPIES	ORGANIZATION
1 ELEC	ADMNSTR DEFNS TECHL INFO CTR ATTN DTIC OCP 8725 JOHN J KINGMAN RD STE 0944 FT BELVOIR VA 22060-6218	1	GENERAL TECHNICAL SERVICES ATTN G P MEISSNER 3100 ROUTE 138 WALL NJ 07719
1	DARPA MTO ATTN N DHAR 3701 NORTH FAIRFAX DR ARLINGTON VA 22203-1714	43	US ARMY RSRCH LAB ATTN IMNE ALC HRR MAIL & RECORDS MGMT ATTN RDRL CIO LL TECHL LIB ATTN RDRL CIO MT TECHL PUB ATTN RDRL SEE A RUGEL-EVANS ATTN RDRL SEE D SEELEY ATTN RDRL SEE E SYVRUD ATTN RDRL SEE G SIMONIS ATTN RDRL SEE G WOOD ATTN RDRL SEE I F SEMENDY (5 HCS) ATTN RDRL SEE I G BRILL ATTN RDRL SEE I G SUN ATTN RDRL SEE I H HIER ATTN RDRL SEE I J LITTLE ATTN RDRL SEE I K K CHOI ATTN RDRL SEE I K OLVER ATTN RDRL SEE I K SABLON-RAMESEY ATTN RDRL SEE I N DHAR ATTN RDRL SEE I P FOLKES ATTN RDRL SEE I P TAYLOR ATTN RDRL SEE I P UPPAL ATTN RDRL SEE I P WIJEWARNASURIYA (10 HCS) ATTN RDRL SEE I S SVENSSON ATTN RDRL SEE I U LEE ATTN RDRL SEE I W BECK ATTN RDRL SEE I W SARNEY ATTN RDRL SEE I Y CHEN ATTN RDRL SEE J ELLER ATTN RDRL SEE K MAJOR ATTN RDRL SEE L BLISS ATTN RDRL SEE P GILLESPIE ADELPHI MD 20783-1197
1	US ARMY RSRCH DEV AND ENGRG CMND ARMAMENT RSRCH DEV & ENGRG CTR ARMAMENT ENGRG & TECHNLOGY CTR ATTN AMSRD AAR AEF T J MATTS BLDG 305 ABERDEEN PROVING GROUND MD 21005-5001		
1	ARMY RESEARCH OFFICE ATTN RDRL ROE L W CLARK III PO BOX 12211 RESEARCH TTRIANGLE PARK NC 27709		
2	CECOM NVESD ATTN AMSEL RD NV A SCHOLTZ ATTN AMSEL RD NV D BENSON 10221 BURBECK RD STE 430 FT BELVOIR VA 22060-5806		
1	US ARMY INFO SYS ENGRG CMND ATTN AMSEL IE TD A RIVERA FT HUACHUCA AZ 85613-5300		
1	COMMANDER US ARMY RDECOM ATTN AMSRD AMR W C MCCORKLE 5400 FOWLER RD REDSTONE ARSENAL AL 35898-5000		
1	US GOVERNMENT PRINT OFF DEPOSITORY RECEIVING SECTION ATTN MAIL STOP IDAD J TATE 732 NORTH CAPITOL ST NW WASHINGTON DC 20402		
		TOTAL:	53 (52 HCS, 1 ELECT)

INTENTIONALLY LEFT BLANK.